1. PRF# 57390-ND5
2. Project Title: ZrO2-Based Alternatives to Precious Metal Catalysts for Naphtha Reforming: Kinetics, Mechanism, and Site Requirements for (cyclo)Alkane Dehydroaromatization
3. P.I. Name, Affiliation: Aditya Bhan, University of Minnesota
4. Co-PI (if any), Affiliation: N/A

Dehydroaromatization (DHA) provides an attractive thermochemical route for CH_4 valorization in reference to indirect and oxidative routes that bring forth significant kinetic challenges in conferring high selectivity.[1] Non-oxidative conversion of CH_4 by pyrolysis reactions to produce aromatics (benzene; at ~70% carbon selectivity) occurs with near equilibrium yield ($6CH_4 \leftrightarrow C_6H_6 + 9H_2$; ~10% single pass conversion) on carbidic forms of Mo encapsulated in zeolites at temperatures ~950 K.[2] Oxidic precursors of Mo deposited in H-ZSM-5 zeolitic channels via vapor phase solid state ion exchange result in formulations that catalyze CH_4 DHA at 950 – 973 K.[3] We demonstrate interpellet physical mixtures and staged packed-bed configurations of pre-carburized MoC_x/H-ZSM-5 catalyst and Zr, a known H_2 absorbent, lift equilibrium limitations, thereby increasing single-pass methane conversion to ~27% and a concurrent 1.4 – 5.6 fold increase in aromatic product yields while retaining the cumulative product selectivity. A reaction-transport model rigorously accounts for catalyst-absorbent proximity effects through consideration of kinetic, diffusive, and convective length scales. Simulation results demonstrate introduction of zirconium metal enhances net methane pyrolysis rates throughout the catalyst bed and accurately predict benzene yield and effluent H_2 partial pressure for various reactor configurations.

Methane DHA rates were measured employing: (i) a MoC_x/H-ZSM-5 catalyst bed, (ii) an interpellet mixture of MoC_x/H-ZSM-5 and Zr, and (iii) MoC_x/H-ZSM-5 with a succeeding Zr bed. Interpellet physical mixtures showed single-pass conversion as high as ~27%, as depicted in Fig. 1(a). The identity and distribution of products is unaltered upon addition of Zr (Fig. 1(b)), suggesting that the bifunctional reaction pathways of methane pyrolysis were unperturbed by hydrogen removal. Interpellet formulations were partially regenerated by treatment in helium at 973 K, removing all absorbed H_2 and yielding above-equilibrium methane conversion in successive regeneration cycles (Fig. 1(a)).

We developed a kinetic-transport model inclusive to all reactor configurations. The model consists of (1) a differential mole balance in the catalyst bed, (2) a differential mole balance for the Zr bed placed downstream of Mo/H-ZSM-5, (3) approach to equilibrium (η) calculations, (4) dimensionless parameters, and (5) the relevant Danckwerts boundary conditions.

(1) $$\frac{1}{Pe}\frac{d^2y_j}{dx^2} - \frac{dy_j}{dx} - \nu_j Da\, y_{CH_4}(1-\eta) - \delta_{H_2,j} Da_{Zr}\, y_{H_2} = 0.$$

(2) $$\frac{1}{Pe_{Zr}}\frac{d^2y_j}{dx^2} - \frac{dy_j}{dx} - \delta_{H_2,j} Da_{Zr} y_{H_2} = 0.$$

(3) $$\eta = \frac{P_{C_6H_6}^{\frac{1}{6}} P_{H_2}^{\frac{3}{2}}}{P_{CH_4}\, K_{eq}}.$$

(4) $$Da = \frac{kL}{u_s} \qquad Da_{Zr} = \frac{k_{Zr} L_{Zr}}{u_s} \qquad Pe = \frac{u_s L}{D_{eff}} \qquad Pe_{Zr} = \frac{u_s L_{Zr}}{D_{eff}}.$$

(5) $$\frac{1}{Pe}\frac{dy_j}{dx}\Big|_{x=0^+} = y_j(0^+) - y_j(0^-);\ y_j(1^-) = y_j(1^+);\ \frac{1}{Pe}\frac{dy_j}{dx}\Big|_{x=1^-} = \frac{1}{Pe_{Zr}}\frac{dy_j}{dx}\Big|_{x=1^+};\ \frac{1}{Pe_{Zr}}\frac{dy_j}{dx}\Big|_{x=1+\frac{L_{Zr}}{L}} = 0$$

Da and Pe^{-1} reflect ratios of the characteristic convective length-scale to kinetic and diffusive length-scales. Pe and Pe_{Zr} are Péclet numbers in the catalyst and Zr bed, respectively, both taken to be unity per numerical fit while the Damköhler number (Da) for the pseudo 1st-order forward

benzene synthesis rate, was calculated via kinetic investigations. Profiles for benzene yield and approach to equilibrium along the catalyst bed predicted by the kinetic-transport model are in quantitative agreement with the experimental results as shown in Fig. 1(c). The impact of catalyst-absorbent proximity is evident in comparison of benzene yield in cases (ii) and (iii) (Fig. 1(c)). Physical interpellet mixtures of MoC_x/H-ZSM-5 and Zr show the largest maximum benzene yield, but deactivate most rapidly. Intimacy of product formation and scavenging functionalities in interpellet mixtures disproportionately promotes formation of higher aromatics which congest zeolite pores and sterically hinder dehydrocyclization steps. Separation of catalytic sites from H_2 absorptive function mitigates deactivation and increases cumulative benzene yield from 3.03 to 3.78 mol_{C6H6} mol_{Mo}^{-1} at 8.7 ks TOS from case (ii) to case (iii) which correspond to ~2x enhancement relative to MoC_x/ZSM-5.

Impact of the research

Introduction of a continuous H_2 scavenging functionality in interpellet and staged-bed configurations of MoC_x/H-ZSM-5 and Zr lift thermodynamic equilibrium constraints for non-oxidative methane conversion, enhancing aromatic synthesis rates and cumulative product yields without changes to product distribution. Kinetic-transport models and dimensionless parameters quantitatively capture effects of hydrogen absorption and provide a framework to investigate performance of various reactor configurations through the formalism of Da and Pe which capture interplay between kinetic, diffusive, and convective length-scales.

References

1 J. H. Lunsford, *Catal. Today*, 2000, **63**, 165–174.

2 J. Bedard, D. Y. Hong and A. Bhan, *J. Catal.*, 2013, **306**, 58–67.

3 H. S. Lacheen and E. Iglesia, *Phys. Chem. Chem. Phys.*, 2005, **7**, 538–547.

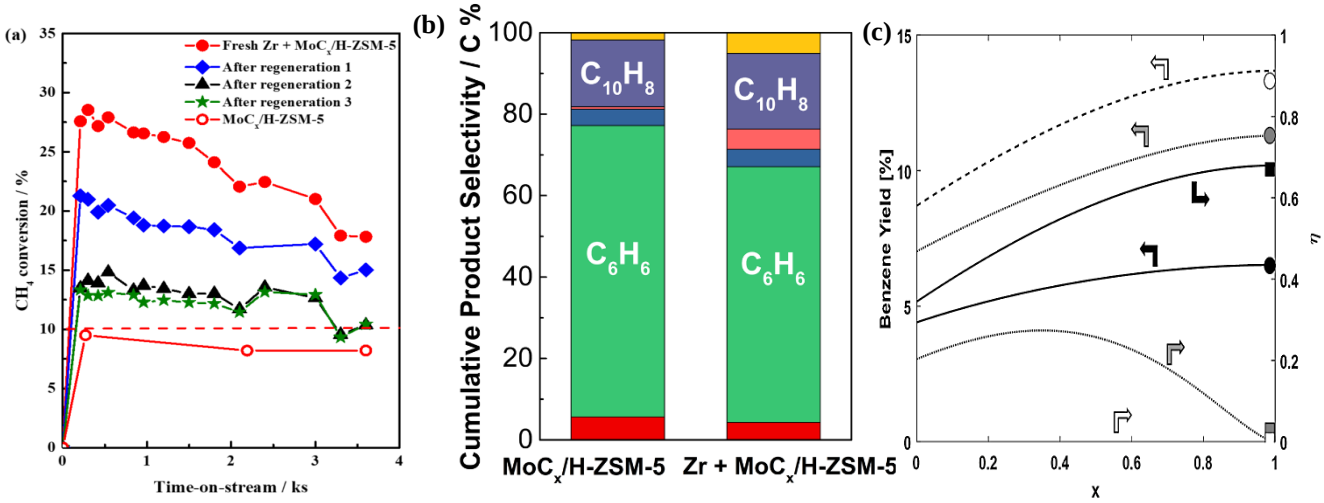

Figure 1: (a) CH_4 conversion vs TOS for case (i) and case (ii) before (fresh) and after regeneration in He flow. Regenerations 1, 2, and 3 by flushing in He flow at 973 K for 61.2 ks, 84.6 ks, and 34.2 ks respectively. Dashed red line indicates ~10% equilibrium conversion. (b) Cumulative product selectivity for case (i) and case (ii), calculated after 8.7 ks TOS. (c) Axial profiles of benzene yield and approach to equilibrium, as predicted by the kinetic-transport model, for cases (i), (ii), and (iii), shown in solid, dashed, and dotted lines, respectively. Measured benzene yield (approach to equilibrium) for cases (i), (ii), and (iii) shown in black, white, and gray-filled circles (squares), respectively. Simulations predict $\eta \rightarrow 0$ throughout the bed for case (ii). MoC_x/H-ZSM-5 ~1.2 g, Zr ~2.4 g, ~0.21 cm^3 s^{-1} (90 vol% CH_4), reaction at ~973 K.